Dual-wavelength FBG inscribed by femtosecond laser for simultaneous measurement of high temperature and strain

Yong Zhu (朱 永)[1*], Hao Mei (梅 浩)[1], Tao Zhu (朱 涛)[1], Jie Zhang (张 洁)[1], and Shizhuo Yin[2]

[1]*Key Laboratory for Optoelectronic Technology & System, Ministry of Education of China, College of Optoelectronic Engineering, Chongqing University, Chongqing 400030, China*

[2]*Department of Electrical Engineering, The Pennsylvania State University, University Park, PA 16802, USA*

[*]*E-mail: yongzhu@cqu.edu.cn*

Received December 1, 2008

A novel fiber Bragg grating (FBG) with two transmission dips in 1310- and 1550-nm regions is proposed and inscribed by an infrared femtosecond laser. Formed by multi-photon ionization, this type of grating can withstand temperature as high as 800 °C which makes it suitable for harsh environment sensing. In addition, the temperature and strain affect these two dips in different ways, which enables simultaneous strain and temperature sensing. The fabrication, spectrum characterization, and temperature performance of this grating are introduced.

OCIS codes: 060.2370, 140.7090, 050.2770.

doi: 10.3788/COL20090708.0675.

Due to their advantages of high sensitivity, high accuracy, and quasi-distributed capability, fiber Bragg grating (FBG) sensors play a more and more important role in structural health monitoring, especially in harsh environment such as aircraft wings, aircraft tanks, bridges, dams, and tunnels[1]. However, the ultraviolet (UV) induced FBG has very poor high temperature stability and cannot withstand a temperature higher than 300 °C. Furthermore, its cross sensitivity to both strain and temperature is also a challenging problem in real world applications. To address these problems, in the past decade, a series of techniques has been proposed for simultaneous temperature and strain measurement using FBG, including dual-wavelength FBG with high order grating diffraction[2], superposed Bragg gratings[3], hybrid Bragg grating/long period grating[4], FBG superposed with polarization-rocking filter[5], superstructure FBG[6], chirped FBG[7], hybrid Bragg grating/Fabry-Perot interferometer[8,9], cascaded FBGs written on different doped fibers[10], and so on. In recently years, the high temperature stability of FBGs has also been strongly improved by the development of infrared (IR) femtosecond laser writing technique[11]. Among all temperature and strain discrimination methods, dual-wavelength FBG is the relatively convenient approach. However, the Bragg wavelengths of the first and high diffraction orders are quite different and may exceed the single-mode wavelength range of ordinary single mode fiber (SMF). For example, a FBG with the first order Bragg wavelength at 1530 nm will have the third order Bragg wavelength at 510 nm, and therefore is not suitable for real sensing system. Zhu *et al*. reported a bending temperature and strain sensor based on multimode FBG induced by an IR femtosecond laser, which has several dips in C-band[12]. Zan *et al*. proposed a temperature and strain sensor based on polarization maintaining FBG inscribed by a femtosecnod laser, which has two dips at 1544 and 1542 nm. However, the polarization maintaining fiber is too expensive for common fiber sensing systems, and the propagating modes in mulit-mode FBG are so complicated that the grating dips in it are not stable enough. To address this problem, in this letter, a novel FBG on common SMF (SM28 from Corning) with two transmission dips at 1310- and 1550-nm regions is proposed and inscribed by an IR femtosecond laser.

To generate a dual-wavelength FBG, two Bragg gratings should be written on fiber simultaneously. Therefore, a near-field phase mask method[14] was adopted instead of point-to-point writing scheme. As shown in Fig. 1, a standard silica SMF is exposed to IR laser pulses of 150-fs duration that are generated by a Quantronix Titan IR femtosecond laser system with a wavelength of 800 nm and a pulse repetition rate of 1 kHz. The laser beam diameter is about 10 mm and is focused by a cylindrical lens with a 38-mm focal length. The phase mask is optimized for 800 nm with a pitch of 2.66 μm, and about 5% of the beam is diffracted into the zeroth order. Multiple interference pattern pitches can be generated due to the involvement of multi-beam interference[11]. The pattern with half of the mask pitch is the result of two-beam interference between +1st and −1st diffraction orders, which has an interferometric visibility of about 100% given by[15]

$$K = \frac{2\sqrt{I_1 I_2}}{I_1 + I_2}, \tag{1}$$

where K is the interferometric visibility, I_1 and I_2 are the intensities of two interference beams. While the pattern with the mask pitch is the result of two-beam interference between the 0th and 1st diffraction orders,

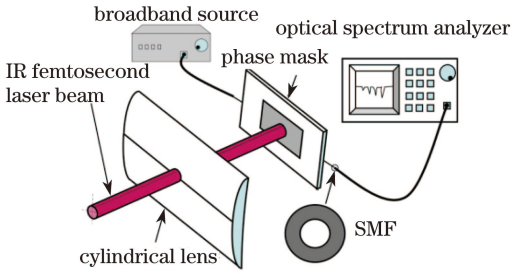

Fig. 1. Schematic diagram of the experimental setup used to fabricate dual-wavelength Bragg gratings in SMF by an IR femtosecond laser.

and has an interferometic visibility of about 59%. Determined by the interferometric visibility of these patterns, the effective diffraction index modulation amplitudes of the two Bragg gratings inscribed by the mask are different. Furthermore, for a practical phase mask, the interferometric visibility also changes with the gap variation between the fiber and the mask[14], so it is critical to carefully adjust the gap to get good dual-pitch gratings. The fiber was placed on a high-precision moving stage, and the optimized gap was set to 200 μm according to our experiments.

Figure 2 shows a microscopic image of a dual-pitch grating fabricated in SMF, which includes the grating pitches of 2.66 and 1.33 μm. These pitches correspond to high-order Bragg grating resonance, given mathematically by

$$2n_{\rm eff}\Lambda_{\rm g} = m\lambda_{\rm Bragg}, \tag{2}$$

where m denotes the diffraction order, $n_{\rm eff}$ represents the effective refractive index for the propagating mode in the SMF, $\lambda_{\rm Bragg}$ is the Bragg resonant wavelength, and $\Lambda_{\rm g}$ denotes the grating pitch. In our experiment, the 2.66-μm grating has the 5th order mode (i.e., m=5) resonant peak around 1535 nm, while the 1.33-μm grating has a 3rd order mode resonant peak around 1286 nm. Assume the two gratings have square wave diffraction index modulation shape, and can be expressed as[16]

$$f(z) = \sum_{n=1}^{m} \frac{\sin[\frac{2\pi}{\Lambda_{\rm g}}(2n-1)z]}{2n-1}, \tag{3}$$

where $f(z)$ is the function of the diffraction index modulation of Bragg grating in SMF, z represents the variable along the z-axis of the fiber, $2n-1$ is the order of harmonic. The 3rd harmonic has a coefficient of 1/3, while the 5th harmonic has a coefficient of 1/5. Therefore, if the diffraction index modulation depths of both pitches are the same, the 1286-nm resonant due to the 3rd order diffraction is stronger than the 1535-nm peak of the 5th order diffraction. For this reason, to get a balanced dual-wavelength Bragg grating, it is critical to control the exposure time.

In our experiments, the pulse energy is set to 1.5 mJ/pulse, which is strong enough to inscribe type II IR gratings[11]. As a result, the 3rd order peak of 1.33-gμm pitch grows faster than the 5th order one of 2.66-μm pitch. Figure 3(a) is the transmission spectra of 1.33-μm pitch of one dual-wavelength FBG, with the exposure time of 0.5 s (500 pulses). The 3rd order peak of 1.33-μm pitch reaches to a maximal value, and after that, erasure occurs due to over exposure. For an addition 0.125-s exposure, the grating starts to be erased, and continuous exposure of another 0.5-s will cause the total erasure of the grating and damage of the fiber. However, for the fifth order grating of 2.66-μm pitch, 0.5-s exposure time

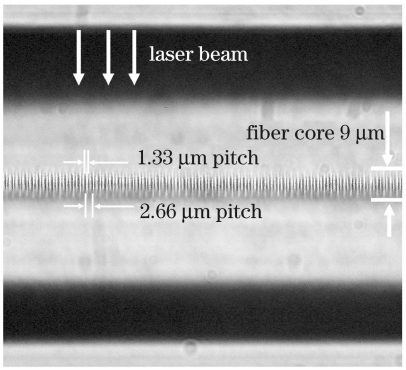

Fig. 2. Microscopic image of an asymmetric FBG fabricated in silica SMF by an IR femtosecond laser with 150-fs, 800-nm laser pulses and a phase mask with 2.66-μm pitch.

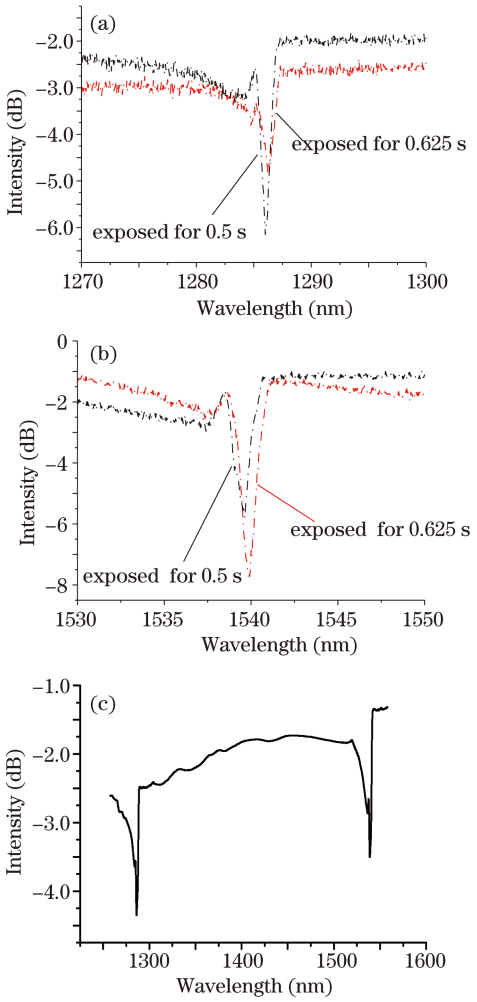

Fig. 3. Transmission spectra of a Bragg grating in silica SMF inscribed by an IR femtosecond laser. (a) Third order diffraction dips of 1.33-μm pitch around 1286 nm; (b) fifth order diffraction dips of 2.66-μm pitch around 1535 nm; (c) a dual-wavelength FBG with the exposure time of 0.5 s.

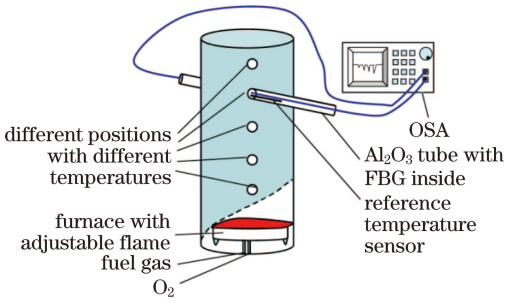

Fig. 4. Schematic diagram of the high temperature experimental setup.

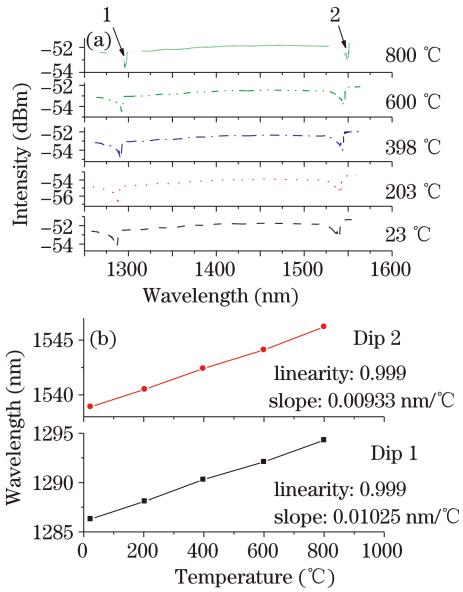

Fig. 5. (a) Spectra of a FBG in a SMF inscribed by an IR femtosecond laser measured at 23−800 °C. (b) Dip location as a function of temperature for two dips.

only results in a 5-dB dip (see Fig. 3(b)). After another 0.125-s exposure, the grating depth is observed increasing to the highest peak depth, and then starts to erase too, and continuous exposure for another 0.5 s will also cause the total erasure of the grating. To get a balance of the 3rd and 5th grating dips, 0.5-s exposure was adopted to write the dual-wavelength Bragg grating in our experiment. The transmission spectrum is shown in Fig. 3(c).

According to Eq. (2), the first dip at 1286 nm and the second dip at 1535 nm have effective refractive indices of 1.4504 and 1.4427 at room temperature. Using these parameters, one can calculate the thermal and strain sensitivity of the dual-wavelength FBG, and then discriminate the temperature and strain effects applied to the sensor as reported before[2]. In our experiment, the high temperature sensing ability is the most concerned. To verify this, we conducted the high temperature sensing experiment, and the dual-wavelength FBG was put in an Al_2O_3 tube and inserted into a furnace. As shown in Fig. 4, the temperature could be changed by inserting the tube into different positions of the furnace as well as adjusting the flame of the furnace. One end of the fiber was connected to an optical spectrum analyzer (OSA, HP 70951), and the other end was connected to the built-in broadband white light source within the OSA.

The spectra of the FBG sensor were measured at different temperatures. Figure 5(a) shows the measured spectra of a FBG at the temperature range of 23 − 800 °C. Along with the increase of temperature, the spectrum shifted, but the spectral profile remained almost unchanged. Figure 5(b) depicts the location as a function of temperature for the two dips. In both curves, the linearity between the dip location and temperature is 0.999, but the slopes of them are different, the 3rd order dip has the slope of 0.01025 nm/°C and that of 5th order dip is 0.00933 nm/°C. This again confirms the high temperature sensing ability of the dual-wavelength FBG as well as the temperature and strain discrimination ability. Although the concept of using dual-wavelength FBGs with high order diffraction inscribed by UV illumination for temperature and strain sensing has been previously studied[2], we report a new type of dual-wavelength FBG in SMF inscribed by an IR femtosecond laser, which offers the new advantage of sensing at high temperature (up to 800 °C). Furthermore, as its Bragg wavelengths are within the single-mode wavelength range of ordinary SMFs (i.e., 1310- and 1550-nm regions), common broadband light source such as light emitting diode (LED) at these wavelength ranges can be used, and ordinary passive SMF components can be adopted to construct a real-world application system. This will significantly reduce the cost of FBG high temperature and strain sensing system.

In conclusion, we have proposed and developed a strain and high temperature sensor based on FBGs fabricated in SMFs by an IR femtosecond laser. The unique capability of simultaneously sensing high temperature and strain is enabled because this novel FBG has the following key features: 1) the FBG could work at high temperature (up to 800 °C); 2) the FBG has two Bragg wavelengths which are within the single mode wavelength range of ordinary SMFs; 3) these two Bragg wavelengths have different effective refractive indices, and the temperature and strain affect them in different ways. This dual-wavelength FBG could be a very good candidate in harsh environment sensing when high temperature and strain co-exist.

This work was supported by the National Natural Science Foundation of China (No. 60707010) and the Natural Science Foundation of Chongqing (CSTC, 2007BB3125).

References

1. F. K. Chang, (ed.) *Structural Health Monitoring 2000* (Technomic Publishing, Lancaster, 1999).
2. G. P. Brady, K. Kalli, D. J. Webb, D. A. Jackson, L. Reelie, and J. L. Archambault, IEE Proc. Optoelectron. **144,** 156 (1997).
3. M. G. Xu, J.-L. Archambault, L. Reekie, and J. P. Dakin, Electron. Lett. **30,** 1085 (1994).
4. H. J. Patrick, G. M. Williams, A. D. Kersey, J. R. Pedrazzani, and A. M. Vengsarkar, IEEE Photon. Technol. Lett. **8,** 1223 (1996).
5. S. W. James, M. L. Dockney, and R. P. Tatam, Electron. Lett. **32,** 1133 (1996).
6. B.-O. Guan, H.-Y. Tam, X.-M. Tao, and X.-Y. Dong, IEEE Photon. Technol. Lett. **12,** 675 (2000).
7. J. Zhang, C. Yu, K. Wang, and J. Zeng, Acta Opt. Sin.

(in Chinese) **28,** 779 (2008).
8. W.-C. Du, X.-M. Tao, and H.-Y. Tam, IEEE Photon. Technol. Lett. **11,** 105 (1999).
9. X. Liao, Y. Rao, Z. Ran, and H. Deng, Chinese J. Lasers (in Chinese) **35,** 884 (2008).
10. P. M. Cavaleiro, F. M. Araújo, L. A. Ferreira, J. L. Santos, and F. Farahi, IEEE Photon. Technol. Lett. **11,** 1635 (1999).
11. C. W. Smelser, S. J. Mihailov, and D. Grobnic, Opt. Express **13,** 5377 (2005).
12. Z. Yong, C. Zhan, J. Lee, S. Yin, and P. Ruffin, Opt. Lett. **31,** 1794 (2006).
13. C. Zhan, J. Lee, S. Yin, P. Ruffin, and J. Grant, J. Appl. Phys. **101,** 053110 (2007).
14. C. W. Smelser, S. J. Mihailov, D. Grobnic, P. Lu, R. B. Walker, H. Ding, and X. Dai, Opt. Lett. **29,** 1458 (2004).
15. M. Born and E. Wolf, *Principles of Optics* (7th edn.) (Cambridge University Press, Cambridge, 1999).
16. A. V. Oppenheim, A. S. Willsky, and S. H. Nawab, *Signal and Systems* (2nd edn.) (Prentice Hall, Englewood Cliffs, 1997).